

Longitudinal Variability of the Vertical Drift Velocity Inferred from Ground-Based Magnetometers and C/NOFS Observations in Africa

Messanga Etoundi Honoré^{1,2,3*}, Paul Obiakara Amaechi⁴, Augustin Daïka^{3,5}, Diaby Kassamba Abdel Aziz⁶, Mohamed Kaab^{7,8}, César Biouele Mbané³, Zouhair Benkhaldoun⁷

¹Department of Geomatics, Higher Technical Teacher Training College of Ebolowa, University of Ebolowa, Ebolowa, Cameroon

²Applied Biotechnology and Engineering Laboratory, Higher Technical Teacher Training College of Ebolowa, Ebolowa, Cameroon

³Laboratory of Earth's Atmosphere Physics, Faculty of Science, University of Yaoundé 1, Yaoundé, Cameroon

⁴Cardiff School of Education & Social Policy, Cardiff Metropolitan University, Cyncoed Campus, Cardiff, UK

⁵Department of Meteorology and Climatology, National Advanced School of Engineering, University of Maroua, Maroua, Cameroon

⁶Laboratoire de Physique de l'Atmosphère, UFR-SSMT, Université Félix Houphouët Boigny, Abidjan, Côte d'Ivoire

⁷Oukaimeden Observatory, LPHEA, FSSM, Cadi Ayyad University, Marrakech, Morocco

⁸National School of Applied Sciences of Beni Mellal, Sultan Moulay Sliman University, Beni Mellal, Morocco

Email: *honormess@yahoo.fr

How to cite this paper: Honoré, M.E., Amaechi, P.O., Daïka, A., Aziz, D.K.A., Kaab, M., Mbané, C.B. and Benkhaldoun, Z. (2022) Longitudinal Variability of the Vertical Drift Velocity Inferred from Ground-Based Magnetometers and C/NOFS Observations in Africa. *International Journal of Geosciences*, 13, 657-680.

<https://doi.org/10.4236/ijg.2022.138035>

Received: July 4, 2022

Accepted: August 22, 2022

Published: August 25, 2022

Copyright © 2022 by author(s) and Scientific Research Publishing Inc. This work is licensed under the Creative Commons Attribution International License (CC BY 4.0).

<http://creativecommons.org/licenses/by/4.0/>



Open Access

Abstract

This study aims at discussing longitudinal effects on the variability of the vertical $E \times B$ drift velocity at low latitudes, specifically over African sector. To this effect, observations from ground-based magnetometers and the Ion Velocity Meter experiment onboard C/NOFS satellite are analyzed in conjunction with equatorial electric field and neutral wind model estimates under geomagnetically quiet conditions in the years 2012-2013. Notwithstanding the limitation in data over Africa, the combination of ground-based and in-situ observations confirmed the existence of longitudinal differences in the $E \times B$ between the Atlantic, Western and Eastern African sectors. This was well reproduced by the equatorial electric field model (EEFM) which showed that during noon, the peak of the equatorial electric field (EEF) was the lowest in the Atlantic sector, with an increasing trend towards the Eastern longitude. The Horizontal Wind Model 14 (HWM14) showed that the eastward zonal (poleward meridional) wind velocity was the lowest (highest) in the Eastern sector. Furthermore, the zonal (meridional) wind increased (decreased) from the Eastern to the Atlantic sector. These results highlight the contribution of the neutral wind velocity in driving the longitudinal difference in the vertical

drift velocity over Africa.

Keywords

Equatorial Electrojet, Vertical Drift Velocity ($E \times B$), Longitudinal Variability, African Sector

1. Introduction

The ionospheric F-region is roughly located between 200 to 800 km in altitude with its daytime plasma distribution determined by mechanism such as production, loss and transport of ions [1]. At low-latitude, the eastward daytime electric field interactions with the horizontal geomagnetic field (H) resulting in the uplift of plasma. The lifted plasma under the influence of gravity and pressure gradient diffuses on both sides of the magnetic equator given rise to the Equatorial Ionization Anomaly (EIA) [2]. The morphology of the anomaly hence, its asymmetry is further affected by neutral wind [3].

The main physical mechanism that accounts for the diurnal variation of the EIA is the fountain effect which itself is driven by the vertical $E \times B$ drift (V_z). Measurements of the vertical plasma drift by the radar at the Jicamarca Radio Observatory (JRO) Peru, showed that V_z exhibits a wide day-to-day variability [4]. This extreme variability has a direct bearing on the distribution of plasma density over EIA, hence on the location and magnitude of the EIA crests as well as the formation of post sunset equatorial ionospheric irregularities [5]. This in turn can impact adversely critical Global Navigation Satellite System (GNSS) operating over the low-latitude region [6] [7].

The deployment of Global Positioning System (GPS) and magnetometers over Africa has provided an unprecedented opportunity to improve our understanding of the electrodynamics that governs the equatorial ionosphere over this region. In effect, while the magnetometers provide information the Equatorial Electrojet (EEJ) and the vertical drift of plasma in the F region [8], the GPS inform us about the structure of the plasma at low or mid-latitude. The combination of these observations is crucial in enhancing our understanding of the complex mechanism modulating the equatorial ionosphere in Africa. It is also crucial in confirming the results obtained by satellite and those predicted by existing models. Magnetometer data, mainly the horizontal component of the geomagnetic field (H) have further proven to be useful in determining the equatorial electrojet (EEJ), a measure of V_z . The EEJ is a current system flowing from West to East in the E-region (100 - 120 km altitude) during the day in a relatively narrow band ($\pm 3^\circ$ magnetic latitude) centered on the magnetic equator [4].

The EEJ strength is determined by the difference in the magnitude of H between a magnetometer placed directly at the magnetic equator and another placed outside (6° to 9° relative to the equator magnetic). Following this approach, [9] estimated the vertical drift from magnetometers at Trivandrum (8.5°N , 77.0°E , 0.5°S

dip lat.) and Alibag (18.5°N, 72.9°E, 13.0°N dip lat.) and showed that large EEJ value during the day was associated with the presence of the crests while weak EEJ was accompanied by the absence of the crests at $\pm 15^\circ$ dip latitude. Reference [10] separated the magnetic contribution from the EEJ by subtracting the magnetic field measured at the station outside the magnetic equator from that measured at the station located at the magnetic equator. Reference [11] showed that, the daytime values of vertical $E \times B$ drift velocity are significantly affected by the radio flux F10.7 and thus by the solar cycle. In addition, [12] established a quantitative relationship between the $E \times B$ measured at the Jicamarca radar and the magnetometers data at Canete (0.8°N. dip lat.) and Piura (6.8°N dip lat.) in Peru, during the solar maximum. Later on, [13] established the same relationship over a long period of time with a larger database of drift and magnetometers. Reference [14] submitted that the ΔH values versus Vz relationship at other longitude sectors should be similar to the relationship in the Peruvian longitude sector if the same Sq dynamo wind systems exist and the penetration of high-latitude electric fields to low latitudes is absent [13].

A global knowledge of vertical drift is crucial for improving the accuracy of theoretical models as well as enhancing our understanding of ionospheric processes (electrodynamics) in the low-latitude. Unfortunately, the non-availability of radars over least covered regions such as Africa, the characteristics long-term absence of ionospheric observational tools and the sparse distribution of existing ones over this continent constitutes a major limitation [15] [16]. Even satellites observations which contribute to a better understanding of the variability of the vertical drift are limited in time for a given longitude.

Past studies have however, suggested that there are longitudinal differences in ionospheric parameters over the longitudinal sectors of Africa [17] [18]. This variability to a large extent has been attributed to changes in the vertical drift [7] [19]. The understanding of this variability is however, limited due to the lack of studies over the various longitudinal sectors of Africa.

This work thus, examines the variability of vertical $E \times B$ drift velocity over the Atlantic, Western and Eastern African longitudes. We have utilised a combination of pairs of magnetometers to compute the EEJ, measurements of drift on board the Communications/Navigation Outage Forecasting System (C/NOFS) satellite as well as the equatorial electric field (EEF) derived from the EEF model and neutral wind data obtained from the Horizontal Wind Model 14 (HWM14) during quiet periods of years 2012-2013.

2. Data and Method of Analysis

2.1. Data Sets

In this study, we have utilized the horizontal component of the Earth magnetic field (H) derived from ground-based magnetometers measurements in Africa. The geographic location of the 6 magnetometers along with their distribution into the Atlantic, Western and Eastern sectors is shown in **Figure 1**. The coordinates of the

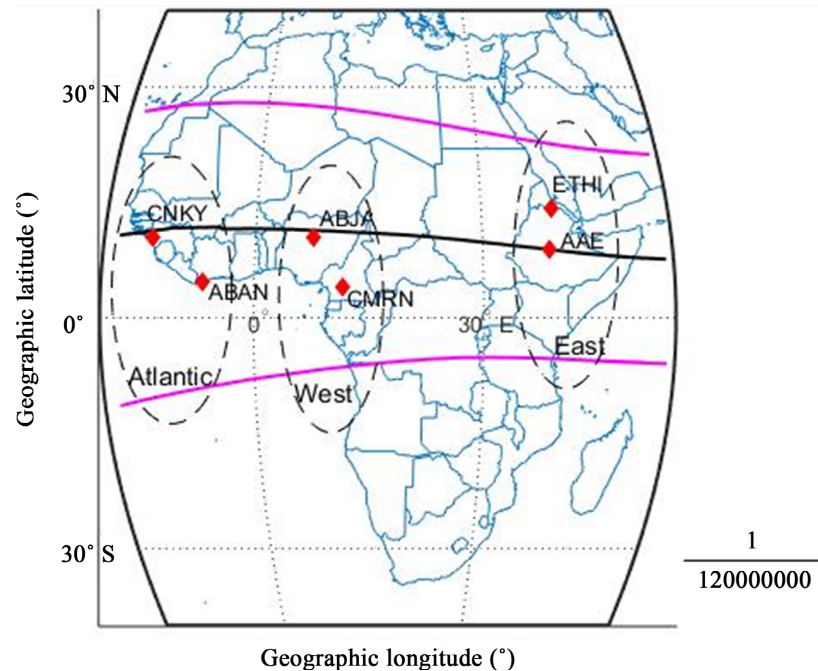


Figure 1. Geographic location of the ground-based magnetometers used. The black solid horizontal line depicts the geomagnetic equator while the two magenta lines indicate $\pm 15^\circ$ dip.

Table 1. Geographic coordinates of the magnetometer stations used.

Station name	Station code	Geographic Latitude	Geographic Longitude	Magnetic Latitude	Magnetic Longitude
Addis Ababa	AAE	9.00°N	38.80°E	0.90°N	110.50°E
Adigrat	ETHI	14.30°N	39.50°E	6.00°N	111.10°E
Abuja	ABJA	10.50°N	7.55°E	0.60°S	79.60°E
Yaounde	CMRN	3.90°N	11.50°E	5.80°S	83.10°E
Conakry	CNKY	10.50°N	13.71°W	2.69°S	60.37°E
Abidjan	ABAN	4.60°N	6.64°W	8.54°S	65.82°E

stations are given in **Table 1**. Data from these magnetometers are provided by the African Meridian B-field Education and Research (AMBER) network except the one in Addis Ababa (AAE) which is made available by the International Real-time Magnetic Observatory Network (INTERMAGNET).

We also utilized $E \times B$ drift (V_z) measurement from the Ion Velocity Meter (IVM), which is one of the Coupled Ion-Neutral Dynamics Investigation (CINDI) sensors on board the C/NOFS [20]. The real time model of ionospheric electric fields was also employed to infer quiet-time equatorial ionospheric electric field as a function of local time for three longitudinal sectors centered along the mean longitude of the pairs of magnetometers. Likewise, we utilized the neutral wind velocities computed from the Horizontal Wind Model 14 (HWM14) [21] over the three longitudes.

As the estimation of $E \times B$ technique, needs pairs of stations, the availability of the magnetic field data of the two ground-based magnetometers for the same quiet day is necessary. All available data sets for the three sectors were obtained during quiet days of years 2012-2013. The five quietest days in each month were obtained from the GFZ German Research Centre for Geosciences.

2.2. Method of Analysis

2.2.1. Estimation of EEJ from Magnetometer Data

The AMBER magnetometers provide geomagnetic data in minutes values of the X , Y and Z components of the magnetic field. In that XYZ coordinate system and by simple geometry, the horizontal component of the geomagnetic field (H) was calculated using the northward (X) and eastward (Y) components according to Equation (1) [22].

$$H = \sqrt{X^2 + Y^2} \quad (1)$$

The nighttime baseline values which correspond to the average midnight values (H_0) of the H component were first calculated for each day and subtracted from the corresponding magnetometer data sets in order to avoid offset values of different magnetometers. The baseline value H_0 is given by Equation (2):

$$H_0 = \frac{H_{23} + H_{24} + H_{01} + H_{02}}{4} \quad (2)$$

where H_{23} , H_{24} , H_{01} and H_{02} are respectively the hourly values of H at 23:00, 24:00, 01:00 and 02:00 in local time (LT). The mean hourly values were computed from the minute interval recorded data of X et Y .

This baseline value is obtained for each day and subtracted from the corresponding magnetometer data sets. Then, the variation of daytime $H_s(t)$ component values of each magnetometer in local time are expressed by the Equation (3):

$$H_s(t) = H(t) - H_0 \quad (3)$$

where s , stand for the relevant station.

Thus, the EEJ current contribution (ΔH) is given by the Equation (4):

$$\Delta H = H_{\text{equator}} - H_{\text{non_equator}} \quad (4)$$

where H_{equator} and $H_{\text{non_equator}}$ are the H measured at the station located at the magnetic equator and off the magnetic equator, respectively.

In this study, the pairs of magnetometers used are Abuja-Nigeria (ABJA) and Yaounde-Cameroon (CMRN); Conakry (CNKY) and Abidjan (ABAN); Addis Ababa (AAE) and Adigrat (ETHI). Abuja, Conakry, Addis Ababa are the ones at magnetic equator and Yaounde, Abidjan, Adigrat off equator.

For each sector, mainly Atlantic, Western and Eastern longitude, Equation (4) is rewritten as in Equations (5)-(7).

$$\Delta H_{\text{Atlantic}} (\Delta H_A) = H_{\text{CNKY}} - H_{\text{ABAN}} \quad (5)$$

$$\Delta H_{\text{Western}} (\Delta H_W) = H_{\text{ABJA}} - H_{\text{CMRN}} \quad (6)$$

$$\Delta H_{\text{Eastern}} (\Delta H_E) = H_{\text{AAE}} - H_{\text{ETHI}} \quad (7)$$

2.2.2. Estimation of Vertical $E \times B$ Drift

The vertical $E \times B$ drift velocity has been estimated using the quantitative relationship [13] as in Equation (8). This relationship between ΔH and $E \times B$ drift is able to infer whether the daytime $E \times B$ drift velocity in the equatorial F-region of the ionosphere is large or small.

$$E \times B = K - \text{TR1} - \text{TR2} - \text{TR3} + \text{TR4} - \text{TR5} + \text{TR6} + \text{TR7} - \text{TR8} \quad (8)$$

where

$K = -1989.51 + 1.002 \times \text{Year} - 0.00022 \times \text{DOY}$, Year is the year of measurements and DOY is the day of the year.

$\text{TR1} = 0.0222 \times \text{F10.7}$, F10.7 is the daily solar flux observed index (in s.f.u);

$\text{TR2} = 0.0282 \times \text{F10.7A}$, F10.7A is the daily solar flux adjusted index (in s.f.u);

$\text{TR3} = 0.0229 \times \text{Ap}$, Ap (nT) is the daily planetary amplitude index;

$\text{TR4} = 0.0589 \times \text{Kp}$, Kp (nT) is the planetary index;

$\text{TR5} = 0.3661 \times \text{LT}$, LT (hours) is the Local time;

$\text{TR6} = 0.1865 \times \Delta H$, ΔH (nT) is the EEJ magnetic effect;

$\text{TR7} = 0.00028 \times \Delta H^2$;

$\text{TR8} = 0.0000023 \times \Delta H^3$.

The technique based on Equation (8) has already been used mostly over the Eastern African longitude [11] [14] [23] [24]. We extend the study to the three longitudinal sectors in Africa and further examine the differences in $E \times B$ between these sectors in line with variations of modelled EEJ values.

2.2.3. $E \times B$ Drift Estimated from C/NOFS Observations (Vz)

We have utilized the C/NOFS IVM sensor to obtain the daytime Vz at the magnetic equator as a function of longitude. Our longitude of interest spanned $15^\circ\text{W} - 45^\circ\text{E}$. Vz can be inferred from the IVM measurements following the approach described in [1] and [7]. This entailed imposing a couple of constraints to the IVM, $E \times B$ drift observations mainly: 1) selecting data from 10:00 to 13:00 LT only since this time window correspond to the maximum $E \times B$ drift velocities over all longitudes; 2) using Vz measurements below 500 km which is low enough to guarantee that O^+ is the dominant ion; and 3) employing data within $\pm 5^\circ$ dip latitude where the magnetic field lines are quasi horizontal. We thereafter averaged IVM observations over each degree of longitude. We recall that only IVM data for the 5 quietest days in a month which satisfied the constraints above were considered from 2012 to 2013.

2.2.4. The Equatorial Electric Field (EEF) Model

The equatorial electric field model uses a transfer function model to predict the variation of EEF from solar wind data and a climatological model to account for the quiet day variations of EEF. It is the climatological component of the model that was used since we were interested in estimating the quiet EEF. We recall that the climatological component of the model uses the quiet time F region

equatorial vertical drift model of Scherliess and Fejer [25]. The input parameters are date, time and location, while the output parameter of interest is the estimated values of EEF. Details about the model can be found in [26]. The model is implemented as a real-time web application

(<http://www.geomag.us/models/PPEFM/RealtimeEF.html>) with ability to harvest real time data, process and archive them.

2.2.5. The Horizontal Wind Model 14 (HWM14)

The zonal and meridional wind velocities were computed following the method described in [27] and [28] (see Equation (9)). This involved estimating the air-glow weighted HWM winds between 200 and 300 km [29].

$$\hat{u} = \frac{\sum_z u_z a_z}{\sum_z a_z} \quad (9)$$

where u_z and a_z are the horizontal winds from the HWM at altitude z and a_z is the redline volume emission rate from Link and Cogger [30] at altitude a_z .

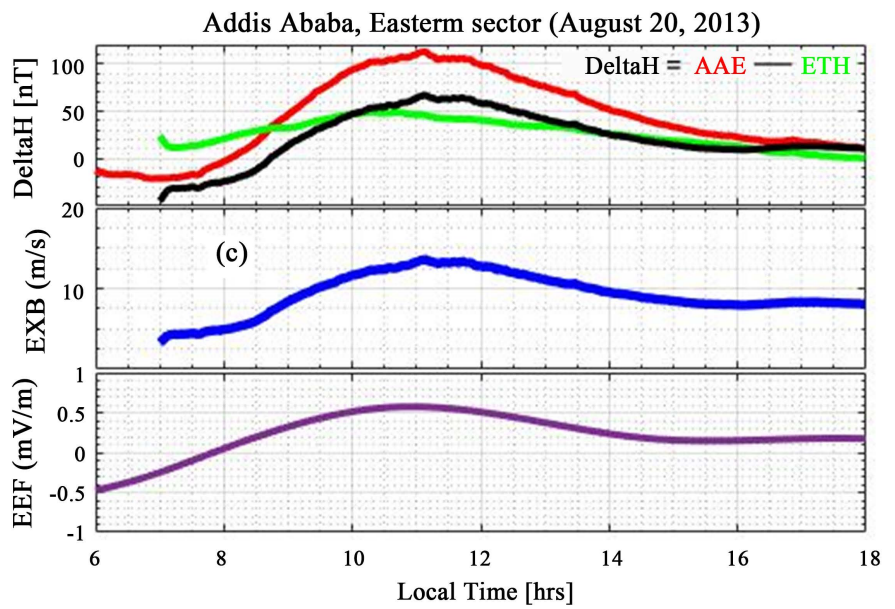
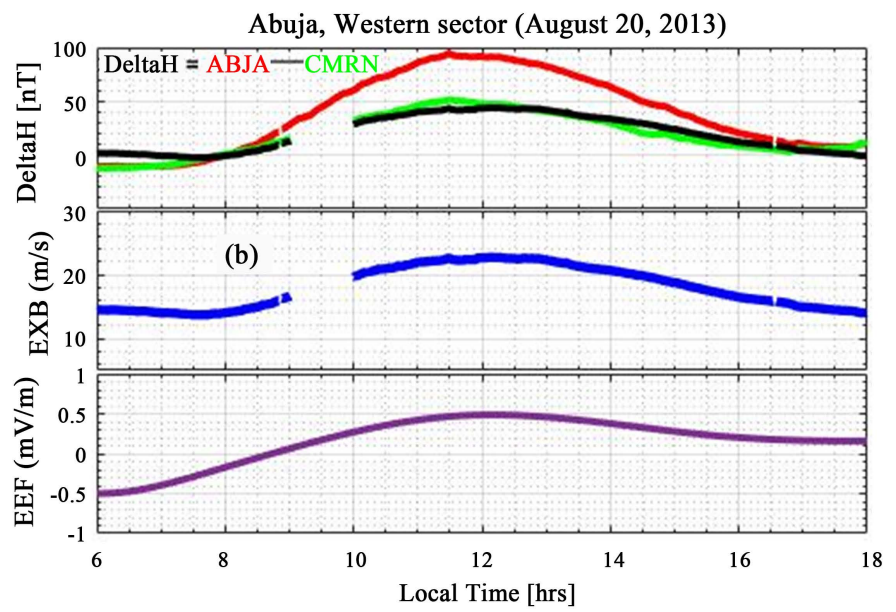
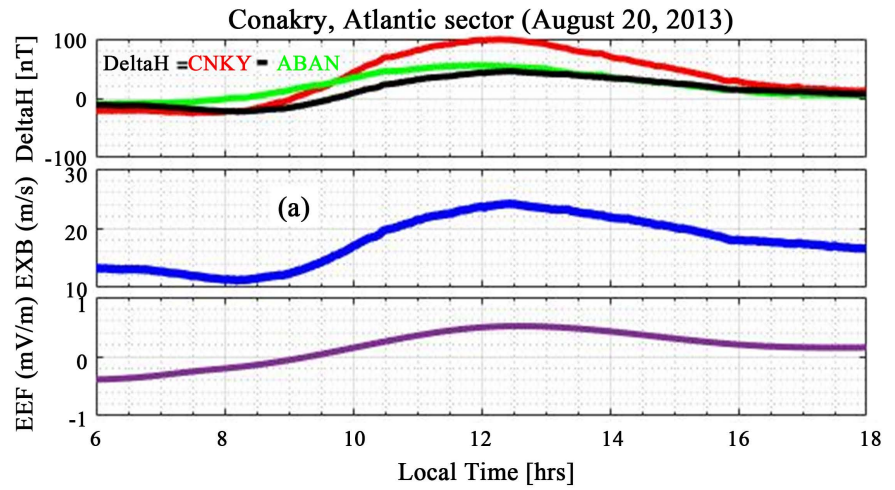
We further computed the seasonal value of the zonal and meridional winds from 06:00-18:00 LT during quiet days over Conakry, Abuja and Addis Ababa each station being located in the Atlantic, Western and Eastern African sector.

3. Results

Figure 2 presents a typical example of daily variations of Delta H (nT) (black curve), vertical $E \times B$ drift velocity (m/s) (blue curve) and EEF (mV/m) (magenta curve) on 20 August 2013 (**Figures 2(a)-(c)**) and 05 September 2013 (**Figures 2(d)-(f)**). These variations have been presented over the stations located in the Atlantic, Western and Eastern African sectors. We however, note that our observations were limited for only these two days where we found data available for all three sectors for the same quiet days.

Generally, the morphology of Delta H was similar to that of the $E \times B$ and EEF over all longitudes. We also observed that ΔH exhibits a significant negative excursion in the morning (6:00 to 8:00 LT). This depression of magnetic field variation in the morning is attributed to a counter-electrojet (CEJ). As can be seen in this figure, CEJ values are a bit lower (-10 nT) in Atlantic and western sectors than that in eastern sector with a value of about -30 nT. According to [31], the CEJ is confined in EEJ and believed to be due to westward current flow within a narrow band near the magnetic equator.

On 20 August 2013 (**Figures 2(a)-(c)**), Delta H, $E \times B$ and EEF reached their respective maximum value of 75 nT, 25 m/s and 0.50 mV/m at about 12:30 LT over the Atlantic and Western sectors. These values were approximately the same over the station in the Eastern sectors. However, the time of occurrence of the peaks was 11:00 LT in this sector. On 05 September 2013 (**Figures 2(d)-(f)**), the time of occurrence of the peak parameters under consideration was 12:00 LT over the three sectors. Nevertheless, the maximum value of Delta H ($E \times B$) was 50 nT (26 m/s), 45 nT (22 m/s) and 70 nT (28 m/s) for the Atlantic, Western and



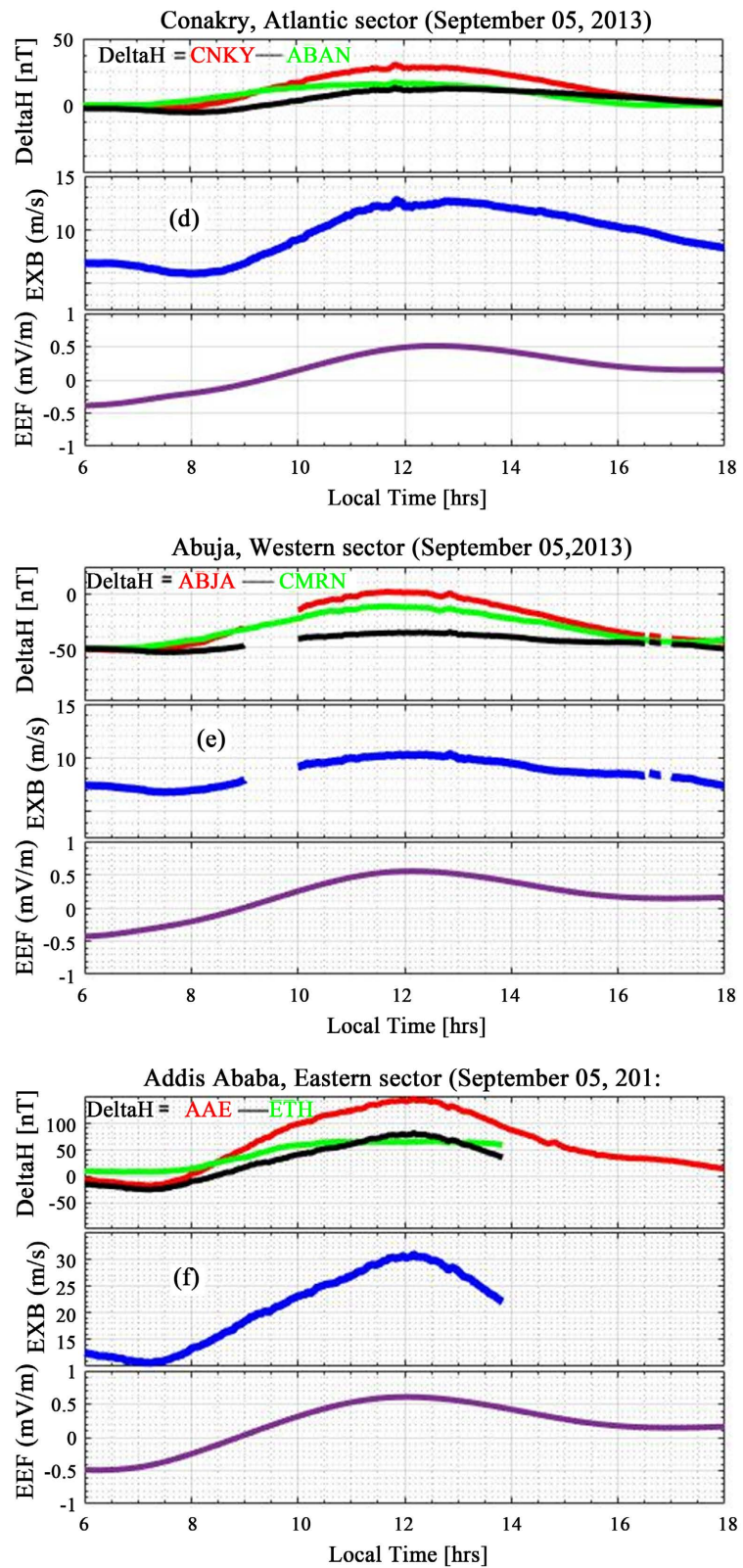


Figure 2. Typical example of the estimated EEJ represented by Delta H (nT) (black curve), vertical $E \times B$ drift velocity (m/s) (blue curve) and EEF (mV/m) (magenta curve) on (a)-(c) 20 August 2013 and (e)-(f) 05 September 2013 over the Atlantic, Western and Eastern African sectors.

Eastern longitude, respectively. The peak values of EEF recorded over these sectors were 0.50 mV/m, 0.55 and 0.60 mV/m.

Figure 3 shows monthly mean variation of Delta H (top panel) and $E \times B$ drift (bottom panel) over (a) Abuja (Western sector) and (b) Addis Ababa (Eastern sector) in 2012. In constructing these Figures, we took the mean of the 5 quietest days in each month to represent the variation for that particular month. It can be seen that Delta H and $E \times B$ exhibited similar monthly variation with peak values occurring at the same time. However, the atlantic sector is not included in, because of the lack of data. Over the Western sector, data was only available in January and February of year 2012. As such both Delta H and $E \times B$ were higher in February than January. Over the Eastern sector, the smallest peak in Delta H and $E \times B$ was occurred in the month of July while the highest peak was observed in March, April and September. The $E \times B$ peak in the month of May was higher than that of January, February and August. Also, the drift reached its peak value earlier in the months of March, April and September (~11:00 LT) and 2 hours late in the month of July (~13:00 LT). Similarly, it reached its peak earlier in February (10:30 LT) and August (11:00 LT) and later in January and May (12:00 LT).

Figure 4 is similar to **Figure 3** but it is for 2013. During this year we had data for 5 months/7 months in the Western/Eastern sector in 2012/2013. Delta H and the $E \times B$ drift varied in a similar manner as in 2012. Over the Western sector, the drift reached its peak value at about 11:00 LT in January and October and latter in August (13:00 LT) and September (14:00 LT). We could not determine the time of occurrence of the peak drift in July due to the data gap. It was also observed that the highest (lowest) drift was registered in the month of August

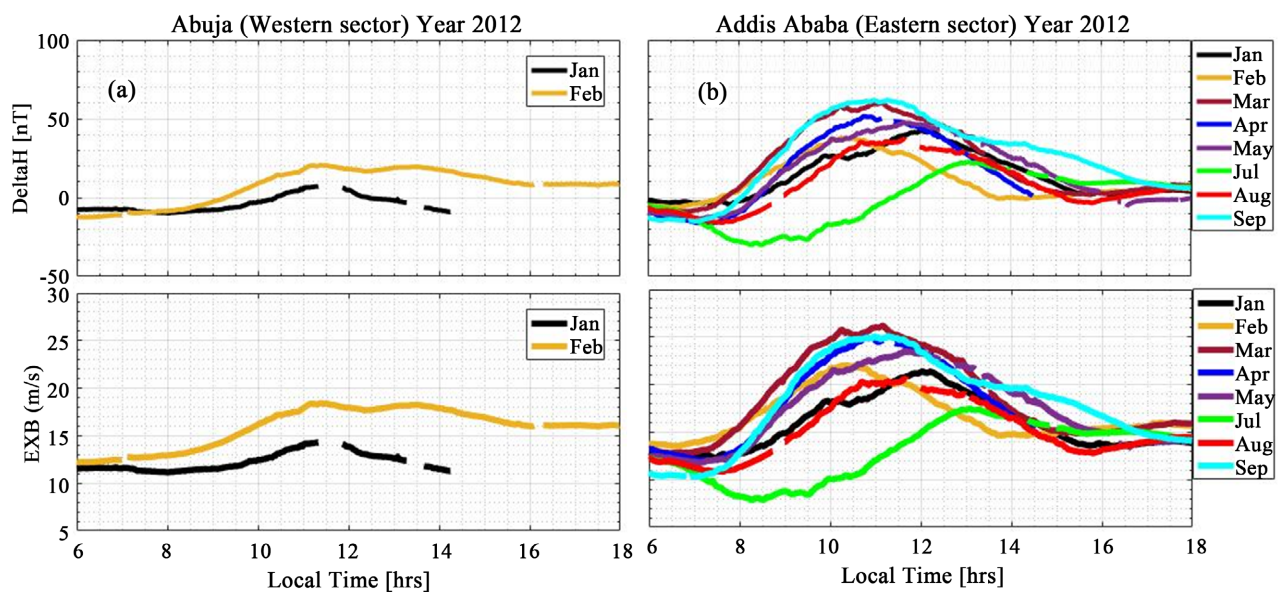


Figure 3. Monthly variation of Delta H (top panel) and $E \times B$ drift (bottom panel) over (a) Abuja (Western sector) and (b) Addis Ababa (Eastern sector) in 2012. Data was only available in January-February in 2012 and January - eptember, excluding the month of June in 2013.

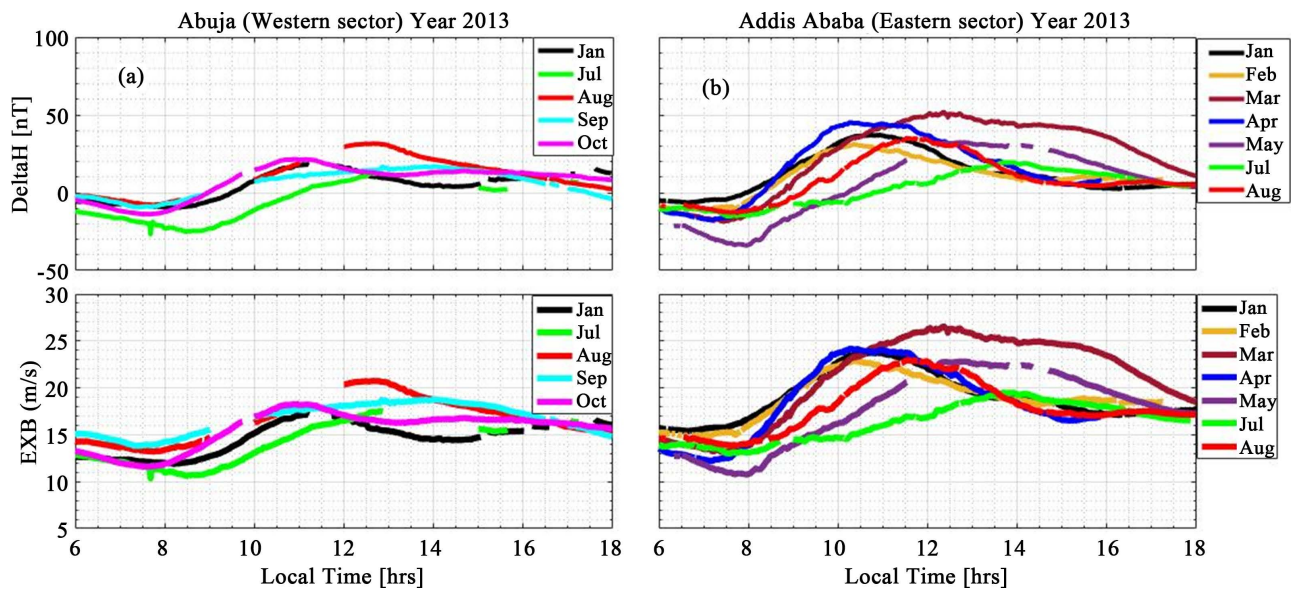


Figure 4. Similar to **Figure 3** but for year 2013. Delta H data was available for 5/7 months in the Western/Eastern sector in 2012/2013.

(January). Over the Eastern sector where data was available for 7 months in the year, the drift reached its peak (lowest) mean monthly value in March (July) at about 12:30 LT (14:00 LT). We also noted the occurrence of earlier peak drift in the months of April/February and January at about 10:30 and 11:00 LT, respectively. Over the Western sector, it was found that the drift was lower in January 2012 (**Figure 3(a)**) than in January 2013 (**Figure 4(a)**). On the other hand, over the Eastern sector, the drift was higher in the months of April, May and July of year 2012 than the corresponding months in year 2013 while it was lower in the months of February, March, than the corresponding months in year 2013. It was nonetheless the same in January and August of both years. As for the time of occurrence of the peaks, in year 2012 (2013), the drift reached its peak at about 11:30 LT (12:30 LT) in March, 12:00 (12:30 LT) in May, and 13:00 (13:45 LT) in July. It however, reached a peak at the same time in February (10:15 UT), August (11:30 UT) of both years. It finally got to its maximum value at 11:00 (10:30 LT) in April, and 12:00 (10:30 LT) in January.

Finally, these mass plots (**Figure 3**, **Figure 4**) give the longitudinal variability of Delta H and $E \times B$ drift which exhibit the difference in magnitude variation. Generally, the magnitude of both elements on March, April, August and September are always greater than those of other months. This is a clear indication that, Delta H and $E \times B$ drift variation exhibit seasonal variation, where both components maximize in equinox.

Figure 5 depicts a typical example of longitudinal variations of the $E \times B$ drift on (a) 20 August 2012 and (b) 5 September 2013 in CNKR (Atlantic sector, green line), ABJA (Western sector, red line) and AAE (Eastern sector, blue line). It compares the magnitude of $E \times B$ drift for the three African sectors. On 20 August 2013, $E \times B$ drift reached a peak of 27 m/s at 11:00 LT in the Eastern sector

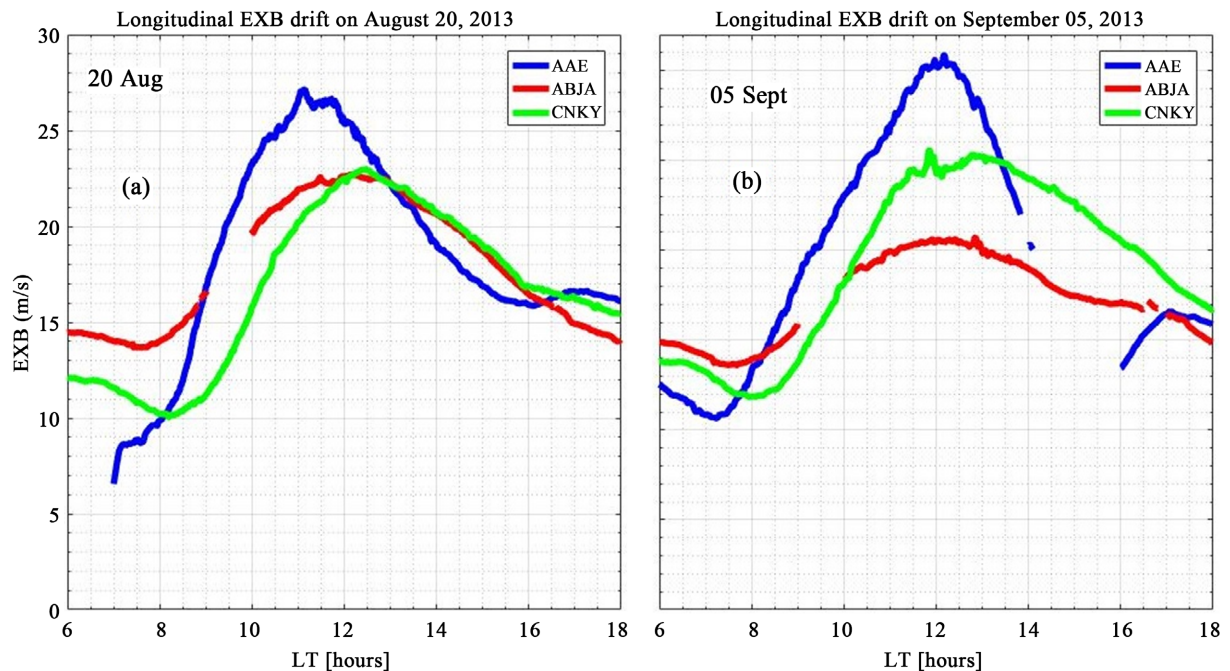


Figure 5. Typical example of daily variation of the $E \times B$ drift over the Eastern (blue line), Western (red line) and Atlantic (green line) sectors on (a) 20 August 2013 and (b) 05 September 2013.

and 23 m/s at 12:30 LT in the Western and Atlantic sectors. On 5 September 2013, the same pattern of variability was observed except with the drift reaching a higher peak of 29 m/s at about 12:00 LT; 19 m/s at about 12:00 LT and 23.5 m/s at 12:00 LT in the Western and Atlantic sector, respectively. This Figure places emphasis on the comparison between observations from ground-based magnetometers and the equatorial electric field on the days when data was available. It was found that the morphology of ΔH was similar to that of the $E \times B$ and EEF over all longitudes. It is shown that, the magnitude of $E \times B$ drift in Eastern sector is greater than that in Western sector.

Figure 6(a) & **Figure 6(b)** present the longitudinal variations of monthly mean $E \times B$ drift over the Eastern (blue line) and Western (red line) during quiet period of year 2012 and 2013. From **Figure 6(a)**, the data were available for January and February 2012 in the Eastern and Western African sectors. In January 2012, the $E \times B$ drift reached a peak of 14.5 (21.5 m/s) at 11:30 (12:00 LT) in Abuja (Addis Ababa). For February, stronger drift values of 18.5 (22 m/s) were obtained over the same stations. The time of occurrence of the peak drift was however, 11:30 and 10:30 LT for Abuja and Addis Ababa, respectively. In **Figure 6(b)**, the drift recorded in January 2013 had increased to 17 m/s and 24 m/s at the respective stations. In July and August 2013, the values were 19.5 m/s and 23 m/s in Addis Ababa. In Abuja, there a data gap in the local noon in July while in August the peak drift was 21 m/s. It was generally observed that the drift in Addis Ababa reached its peak earlier (10:45/11:45 LT) than that in Abuja (11:30/12:30 LT) in January/August 2013.

In **Figure 7**, we display the IVM $E \times B$ drifts velocities (V_z) as a function of

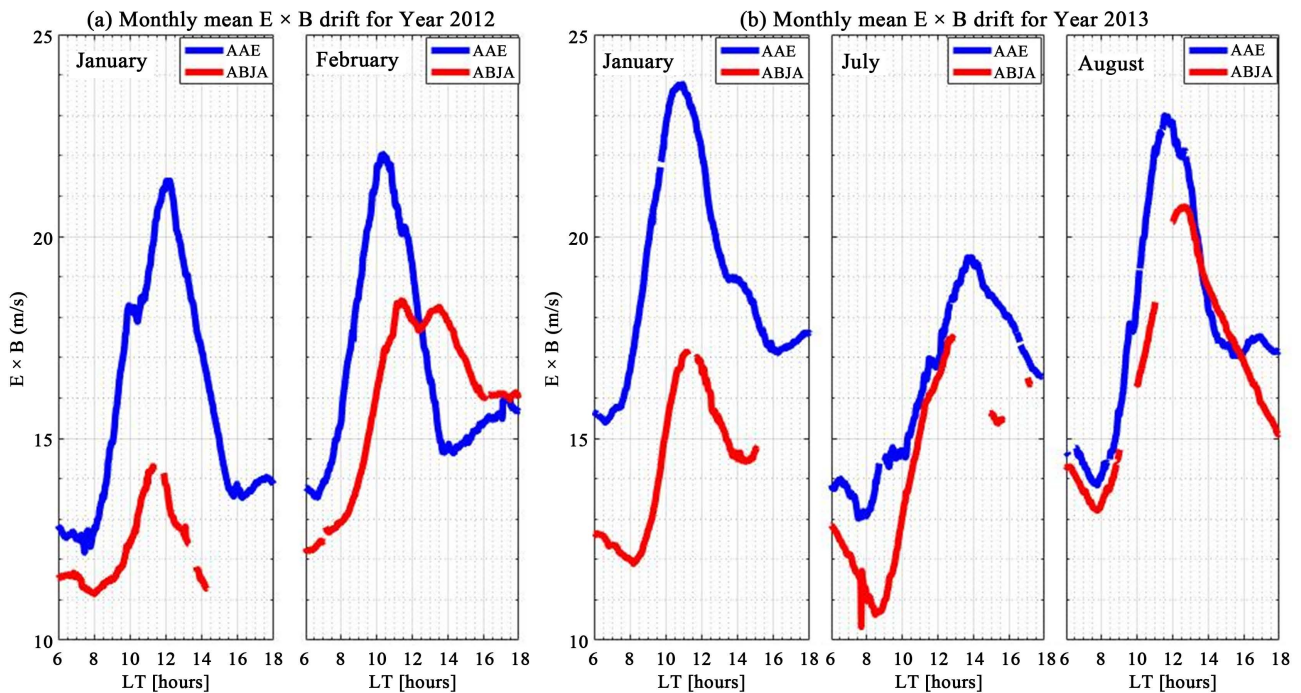


Figure 6. Longitudinal variations of monthly mean $E \times B$ drift over the Eastern (blue line), Western (red line) during quiet period of year 2012 and 2013.

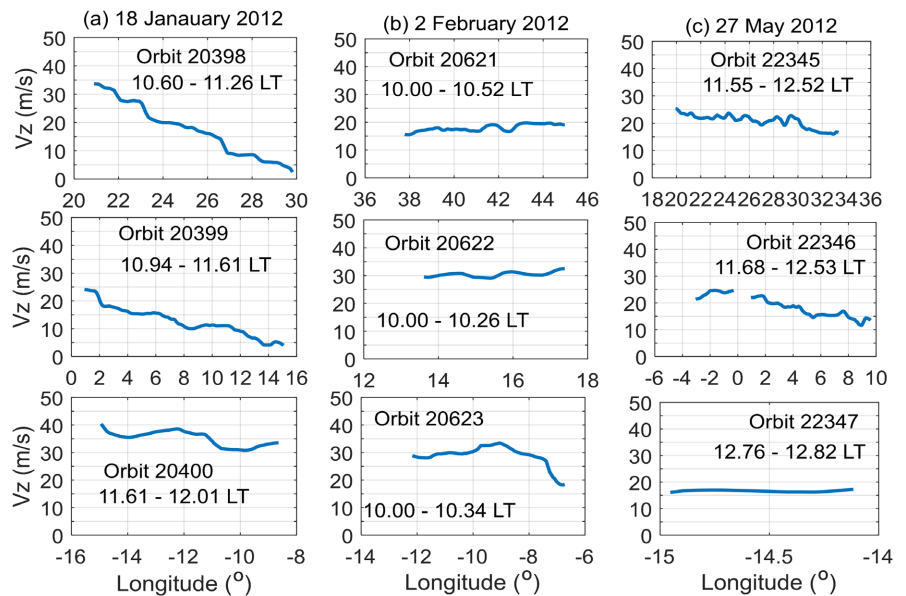


Figure 7. IVM $E \times B$ drifts versus geographic longitude during the quiet days of 18 January, 2 February and 27 May 2012.

geographic longitude for some quiet days when data was available in 2012. **Figure 7** (a) presents the V_z curve during 3 orbits on 18 January 2012 as the satellite covered $16^\circ\text{W} - 30^\circ\text{E}$. During the first orbit (20398), V_z decreased gradually from 34 to 4 m/s within 10.60 - 11.26 LT as the satellite covered longitude $20^\circ\text{E} - 30^\circ\text{E}$ which included the Eastern African sector. There was no sharp longitude gradient in V_z . Similarly, during orbit 20,399, as the satellite covered longitude 0

- 16°E which include the West African longitude, the drift reduced from 28 m/s - 5 m/s within 10.94 - 11.61 LT with no sharp gradient. As the satellite covered the Atlantic sector (16°W - 8°W) during orbit 20400, it measured V_z varying from 40 to 35 m/s within 11.61 - 12.01 LT. From **Figure 7(b)** which deals with the longitudinal variation of V_z from 10.0 - 10.52 LT on 2 February 2012, the satellite covered longitude 38°E - 45°E, 13°E - 17°E and 13°W - 7°W during orbit 20621, 20622 and 20623, respectively. During the respective V_z variation was 15 - 20 m/s, 30 - 33 m/s and 34 - 18 m/s. From **Figure 7(c)**, on 27 May 2012, the satellite covered longitudes 18 - 36°E, 6°W - 10°E and 15 - 14°W during orbits 22345, 22346 and 22347, respectively. The drift varied between 25 - 20 m/s, 25 - 12 m/s and 15 - 17 m/s during the respective orbits.

Figure 8 is similar to **Figure 7** but it shows the drift for quiet days of 3 April, 5 April, 29 October and 12 December 2013. From **Figure 8(a)**, the drift data for orbits 27,012, 27,013 and 27,014 were measured from 10.00 - 11.09 LT as the satellite covered longitudes 28°E - 48°E, 2°E - 22°E and 14°W - 4°W, respectively. The drift varied from 18 - 28 m/s during the first orbit and 26 - 30 m/s during the third orbit. During the second orbit, there was an enhancement in the drift value to a peak of 77 m/s along 9°E at about 10.20 LT. The corresponding value obtained during this local time was 18 m/s at 33°E during the first orbit as against a value of 30 m/s but at 10.37 LT along 14°W. On 5 April 2013 (**Figure 8(b)**), the drift increased gradually from about 2 m/s along 33°E at 10.00 LT to 22 m/s along 45°E at 10.96 LT during orbit 27046. The peak value reached during orbit 27047 was 15 m/s at 10.41 LT along 20°E, and 23 m/s along 14°W at about 10.32 LT. From **Figure 8(c)**, V_z reduced from 13 m/s to 2 m/s within 13.71 - 13.99 LT as the satellite covered 28°E - 33°E during orbit 30,173 on 29

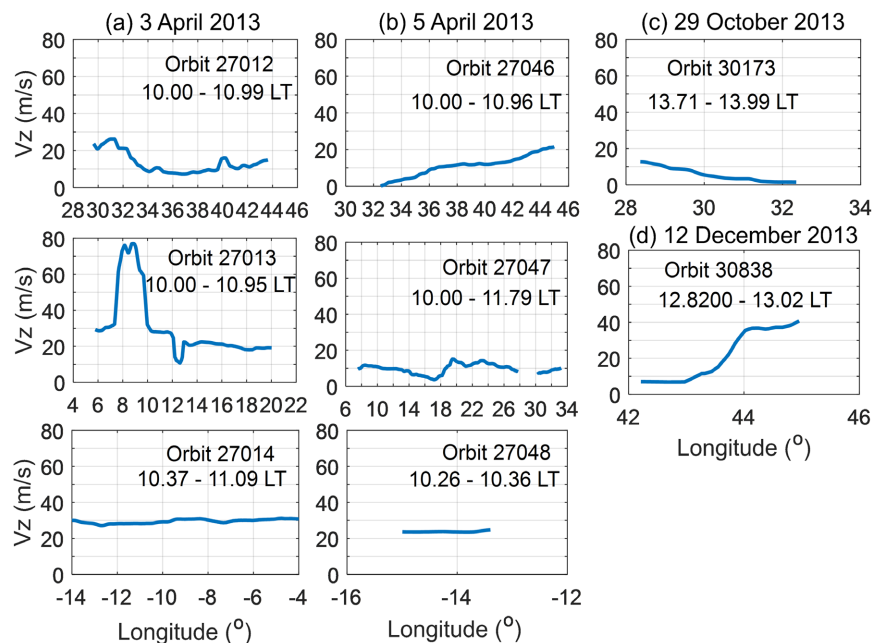


Figure 8. IVM $E \times B$ drifts versus geographic longitude during the quiet days 3, 5 April, 29 October and 12 December 2013.

October 2013. However, on 12 December (**Figure 8(d)**), the satellite covered longitude 42°E - 45°E and V_z increased steadily from 7 - 41 m/s within 12.82 - 13.02 LT.

The results presented in **Figure 7** and **Figure 8** are summarized in **Table 2** which shows the peak and minimum values of the $E \times B$ drift measured by C/NOFS (satellite) over the Eastern, Western and Atlantic sectors.

Figure 9 presents Seasonal variations of equatorial electric field in Africa over Conakry (green line), Abuja (red line) and Addis Ababa (blue line) during quiet period of years 2012 and 2013. These variations have been presented over four seasons: December and June solstices, March and September equinoxes. In general, the EEF variations exhibit the negative excursion in morning (06:00 to 08:00

Table 2. Showing the peak and minimum values of the $E \times B$ drift measured by C/NOFS (satellite) over the Eastern, Western and Atlantic sectors.

Day with data	$E \times B$ drift (m/s)					
	Eastern sector (36°E - 40°E)		Western sector (7°E - 12°E)		Atlantic sector (6°W - 14°W)	
	Max	Min	Max	Min	Max	Min
18/01/2012	-	-	15.5	8	38.6	35
02/02/2012	18.0	15	-	-	33.5	18
27/05/2012	-	-	16.8	12	-	-
03/04/2013	16.0	8	77.0	10	31.0	26
05/04/2013	12.4	10	11.7	9	23.0	21

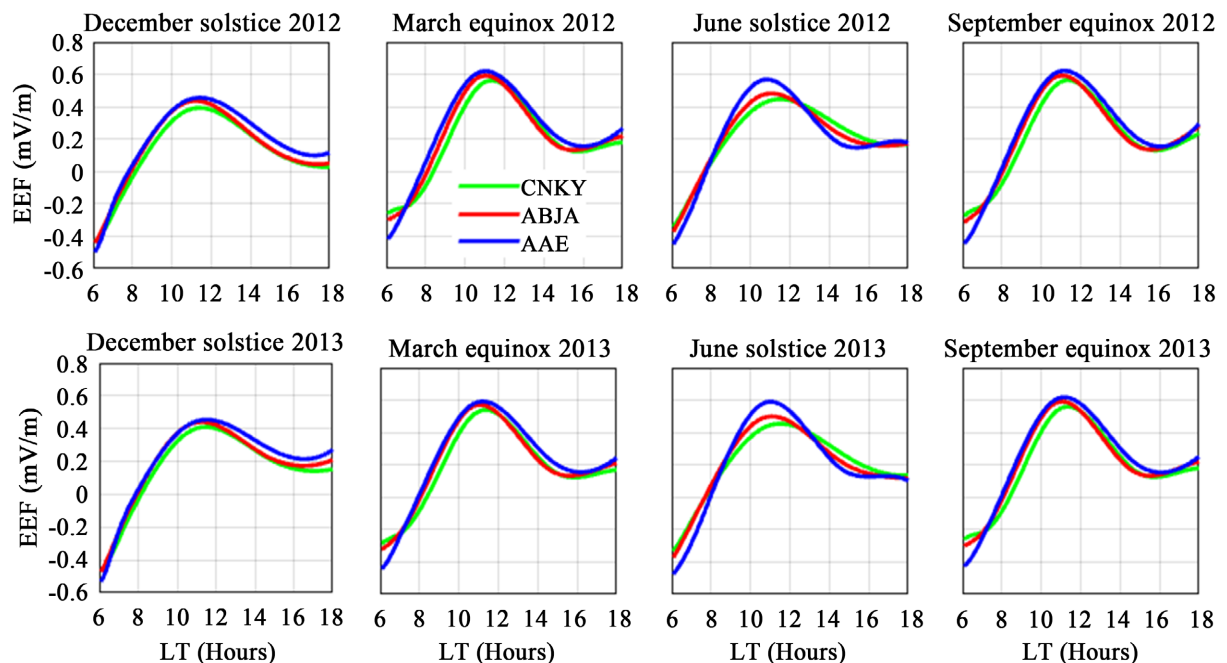


Figure 9. Seasonal variations of equatorial electric field in Africa over Conakry (green line), Abuja (red line) and Addis Ababa (blue line) during quiet period of years 2012 and 2013.

LT) with its maximum observed around 11:00 LT. March and September equinoxes recorded the highest EEF peaks. This was followed by June, then December solstice. Generally, the peak EEF in Conakry was the lowest during all seasons. In June solstice, there was an increase in the peak EEF from Conakry to Abuja and then Addis Ababa.

Figure 10 shows a seasonal variation of quiet time zonal wind derived from the Horizontal Wind Model 14 (HWM14) in 2012 (top panel) and 2013 (bottom panel) over Conakry (green line), Abuja (red line) and Addis Ababa (blue line). From this figure, the zonal wind is essentially negative from 06:00 to 18:00 LT during all the seasons. It reaches its minimum around 15:00 LT and starts increasing until about 18:00 LT. This indicates that the zonal wind is westward within this time window. Generally, the seasonal pattern of the zonal wind was the same in equinoxes and December solstices. However, its magnitude was higher in September equinox. Nevertheless, in June solstice, there was a reversal in the direction of the zonal wind around 09:00 and 15:00 LT. This season also registered the highest zonal wind velocity. We also observed that there was a longitudinal difference in the magnitude of the zonal wind. For example, towards the evening, the wind turned eastward 30 minutes earlier in Addis Ababa and Abuja than in Conakry. Also, its peak velocity was higher in Conakry than at the other stations.

Figure 11 is similar to **Figure 10** but it shows a seasonal variation of quiet time meridional wind derived from the HWM14. There was a striking seasonal difference in the pattern of meridional wind during both years. Equinoxes were mostly marked by poleward wind of weak magnitude (lesser than 24 m/s). However, the wind velocity barely reaching 5 m/s in March equinox while it decreasing

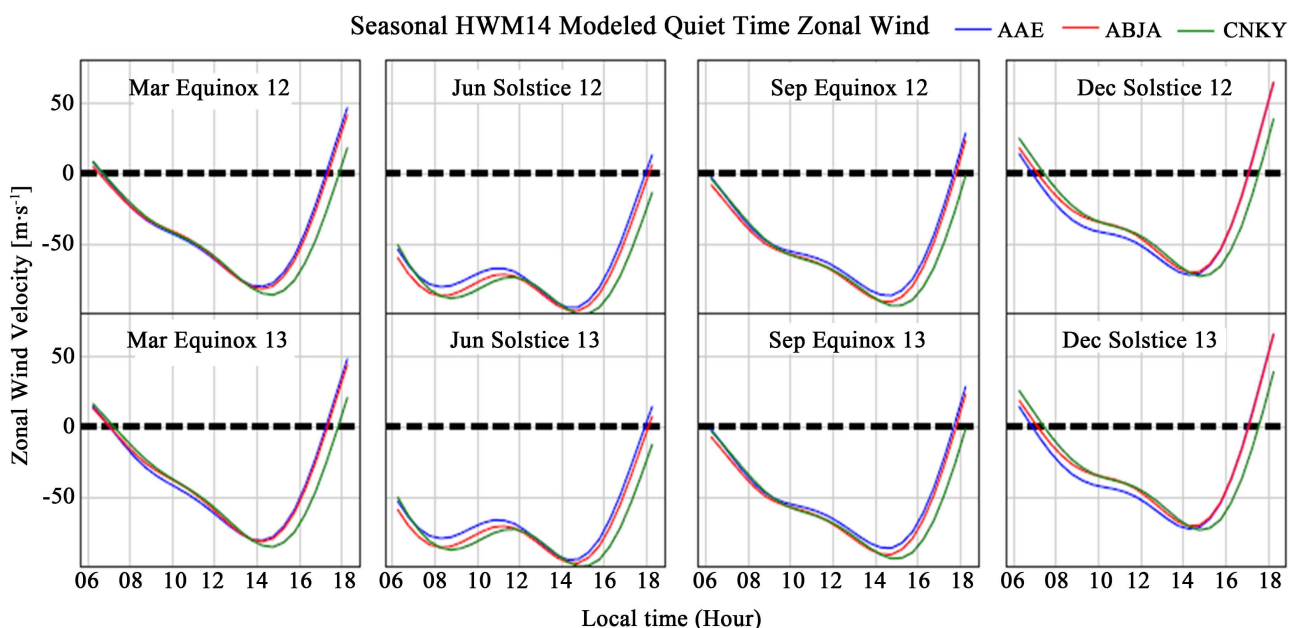


Figure 10. Seasonal variation of quiet time zonal wind derived from the HWM14 in 2012 (top panels) and 2013 (bottom panels) over Conakry (green line), Abuja (red line) and Addis Ababa (blue line).

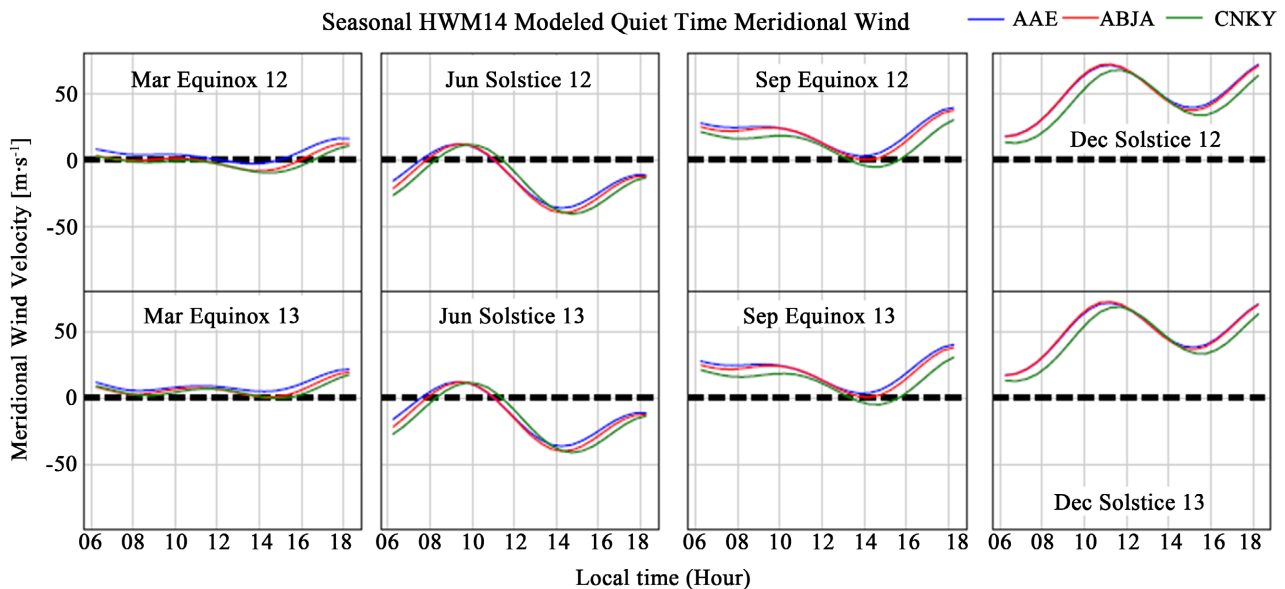


Figure 11. Seasonal variation of quiet time meridional wind derived from the HWM14 in 2012 (top panels) and 2013 (bottom panels) over Conakry (green line), Abuja (red line) and Addis Ababa (blue line).

from a peak 24 m/s to about 0 m/s in September equinox within 10:00-14:00 LT. In December solstice, the essentially poleward wind increased from 06:00 LT to its highest velocity of 80 m/s at about 11:00 LT in Abuja, and 70 m/s at 11:30 LT in Ababa and Conakry. Thereafter it reduced to a minimum at about 14:00 LT. In June solstice, the meridional wind is equatorward with a peak velocity of 42 m/s at about 14:30 LT. However, from 08:00-11:00 LT the meridional wind had reversed to poleward with a peak velocity of 15 m/s. Overall there was a longitudinal difference in with stronger poleward wind in Addis Ababa and Abuja than Conakry in September equinox and December solstice. The poleward (equatorward) wind velocity remained the highest in Addis Ababa (Conakry) in March equinox (June solstice).

4. Discussion

We have examined the variability of V_z over the African equatorial region during quiet periods of years 2012 to 2013. This region has long been avoided of equipment for the direct measurements of drift velocity hence, we adopted the multi-instrument approach which involved the usage of a pairs of magnetometers as well as in-situ satellite data and modelling.

It is well known that the solar quiet (Sq) current system in the E-region is driven by tidal winds gives which rise to the dynamo wind process [32]. The associated current density (J) can be expressed as in Equation (10):

$$J = \sigma \cdot (E + U \times B), \quad (10)$$

where σ is the ionospheric conductivity, E is the electric field, U is the neutral wind, and B is the Earth's main magnetic field. The enhanced conductivity near the magnetic equator results in a strong eastward current known as the EEJ [33].

It has been demonstrated that the EEJ estimated using a pair of magnetometers is a good proxy for the Vz [34] [19]. Unlike past studies which have focussed on a particular sector in Africa, we obtained a good correspondence between the EEJ and vertical $E \times B$ drift (Vz) over the Atlantic, Western and Eastern African sectors. Our results thus, point at the existence of longitudinal difference in the EEJ between the Eastern, Western and Atlantic longitudinal sectors. For example, we obtained differences in the time of peak EEJ and $E \times B$ drift (**Figures 2(a)-(c)**) as well as their peak value (**Figures 2(d)-(f)**) between the Atlantic/Western and Eastern sectors. Interestingly, these longitudinal differences were well captured by the EEFM (see magenta curves of **Figure 2**). As such, an upward drift of 22 m/s, 21 m/s, 28 m/s corresponded to an eastward electric field of about 0.6 mV/m, 0.52 mV/m and 0.70 mV/m for the Atlantic, Western and Eastern longitude, respectively (**Figure 2**). Reference [35] had found that a zonal eastward drift of 100 m/s corresponded with a vertical downward electric field component of magnitude 2.5 mV/m. Notwithstanding the lack of data it could be seen that on monthly basis, Addis Ababa in the Eastern sector had the stronger EEJ and $E \times B$ drifts velocities at least in January and February of year 2012 (**Figure 3**) and in January, July and August 2013 (**Figure 4** and **Figure 6**). Reference [36] for the first time clearly revealed that the western African EEJ appears weaker than eastern EEJ. This discrepancy suggests that there is a process of reinjection of energy in the jet as it flows eastward. This West-East Asymmetrical behavior in the EEJ strength in the African sector is further confirmed by [14] using data set of arrays of magnetometers (AMBER).

The significant negative excursion in EEJ variability that had been observed in the morning (6:00 to 8:00 LT) on **Figure 2**, is attributed to a counter-electrojet (CEJ). As can be seen in this figure, CEJ values are a bit lower (-10 nT) in Atlantic and western sectors than that in eastern sector with a value of about -30 nT. Reference [37] had shown in their study that, the African stations registered the greatest percentage of occurrence of the CEJ than elsewhere. The greatest percentage occurrence of morning CEJ was found at Addis Ababa (eastern Africa) and the greatest percentage of occurrence of afternoon CEJ was found at Ilorin (western Africa).

CNOF/S measurements of Vz also showed the existence of longitudinal difference over Africa (**Figure 7**). For example, the satellite recorded the maximum drift of 40 m/s in the Atlantic (15° W) as against 5 m/s in the Western (15° E) longitude at 11.61 LT, and 4 m/s in the Eastern (30° E) at 11.26 LT on 18 January 2012 (**Figure 7(a)**). Also, on 2 February (**Figure 7(b)**), the peak Vz recorded at 10.18 LT was 34 m/s in the Atlantic sector (9° W), 31 m/s in the Western sector (15° E) and 17 m/s in the Eastern sector (40° E). Similar, in **Table 2**, there were differences in the value of the peak Vz measured over the three sectors during some quiet days of 2013. The combination of ground-based and in-situ observations has therefore clearly confirmed the existence of differences in Vz over the three longitudinal sectors in Africa. We however, noted that our observations

were limited by the lack of data. Our results presented in **Figure 3** and **Figure 4**, show that $E \times B$ drift variation exhibit seasonal variation, where it maximizes in equinox and weaker during the June solstice. The similar trend was also observed in **Figure 9** where September equinoxes recorded the highest EEF peaks. These results are in good agreement with results presented by [14]. Their two independent observations show a consistent seasonal variation with peaks during equinox and weaker during June solstice.

We have thus, resolved to investigate the longitudinal differences on a seasonal basis using the EEFM. It was found that the peak EEF was generally increased from the Atlantic to the Eastern longitude (**Figure 9**). There was a time delay between the occurrence of the peak EEF in Conakry and other stations. Generally, factors such as 1) the difference in magnetic declination [38], 2) irregular changes in the neutral wind caused by meteorological forcing from the lower atmosphere [39], 3) the difference in the magnitude of the horizontal component of the geomagnetic field (B), 4) the offset between the geographic and magnetic equator [40], and 5) the existence of a four-cell longitude pattern in the day-time V_z related with the propagation of wave number 3 (DE3) tidal mode [1] [41] have been identified as potential drivers of the longitudinal difference in V_z . We clearly exclude the existence of DE3 over this sector as there were no sharp gradient in our V_z data. We note that other factors could have played a contributory role in driving the observed longitudinal differences in Africa based on the fact there are obvious difference in magnetic declination (2.21° , -0.28° and -6.3°); B (35,768 nT, 33,698 nT and 31,729 nT), magnetic and geomagnetic offset (9.05° , 11.37° and 11.8°) between Addis Ababa (Eastern sector), Abuja (Western sector) and Conakry (Atlantic sector), respectively. We therefore, believe that the wind might have played a bigger role in modulating these differences.

Our investigation of the seasonal variability of neutral wind at the three stations revealed that during all seasons, the zonal wind is westward with a peak velocity that increased from Addis Ababa to Abuja, and then Conakry at about 14:00 LT (**Figure 10**). Oppositely, the meridional wind is poleward with a velocity that decreased from Addis Ababa, then Abuja and Conakry. From 10:00-14:00 LT in June solstice however, the wind turned to equatorward with a weaker velocity in Conakry (**Figure 11**). We had earlier found that the peak EEF increased from Conakry to Addis Ababa. The meridional (zonal) wind was clearly the strongest (weakest) in Addis Ababa where the electric field was also the strongest of the three sectors. We thus, submit that the electric field was stronger at the longitudinal sector where the zonal wind was minimal and the meridional wind maximal. Reference [42] had stressed on the role of the meridional wind on driving longitudinal difference in the eastward $E \times B$ drift at the equatorial region. They found that the longitudinal variation in the drift was related to the changes in the zonal currents driven by meridional winds at F region height of the equatorial ionosphere. It had been recently found that, changes in the thermospheric neutral winds are the reason for the longitudinal differences that have been re-

ported in equatorial electric fields between the West and East Africa stations [14] [43] [44]. They found that, in general, the neutral wind speed observed in eastern African sector is weaker and stronger in west African sector compared with speeds observed in other longitude sectors.

5. Conclusions

The following points can be taken as the main findings of this study:

1) Satellite observations and ground-based data showed the existence of longitudinal differences in the magnitude of the $E \times B$ drift over the Atlantic, Western and Eastern sectors. These were well reproduced by the EEFM during the days when data were available at the three longitudinal sectors. We note that past works had only focussed on the Western and Eastern sectors.

2) On a seasonal basis, the strongest EEF peak was observed over the Eastern sector suggesting that the vertical drift is also the strongest over that sector. In addition, the trend of variation of EEF showed a reduction in peak from the Eastern sector to the Atlantic sector.

3) There was a longitudinal difference in the magnitude of the zonal wind which was essentially westward from 06:00 to 18:00 LT. Furthermore, the zonal wind velocity was higher at the station located in the Atlantic sector.

4) Overall, there was also a longitudinal difference in poleward meridional wind with its peak velocity being the highest in the Eastern sector. The trend in variation of the meridional wind showed a reduction from the Eastern to the Atlantic sector.

We could infer thus, that the neutral wind had played a crucial role in driving the longitudinal differences in the vertical drift velocity in Africa. The fact that the zonal wind is weaker while the meridional wind is stronger in the Eastern sector could account for the stronger vertical drift velocity measured at this longitude. Direct wind and drift measurements are therefore needed over this region for a better understanding of the equatorial ionospheric dynamics and its morphology and thus, the impact on critical navigation and communication technologies.

Acknowledgements

The authors thank to AMBER (<http://magnetometers.bc.edu>) and INTERMAGNET (<http://www.intermagnet.org>) teams for the magnetometer data they made available to the public. AMBER is operated by Boston College and funded by NASA and AFOSR. We also thank the GFZ Potsdam (<https://www.gfz-potsdam.de>), NOAA Space Weather Prediction Center (SWPC) and the World Data Center (WDC) teams for the geomagnetic and solar activity indices they made available to the public. We thank Ludger Scherliess and Bela Fejer for the Climatological model (<http://geomag.org/models/PPEFM/RealtimeEF.html>). The wind data were derived from the pyglow package, which is an open source software available at <https://github.com/timduly4/pyglow/>.

The authors thank the editor and anonymous reviewers for their help in evaluating this manuscript.

Conflicts of Interest

The authors declare no conflicts of interest regarding the publication of this paper.

References

- [1] Araujo-Pradere, E.A., Anderson, D.N. and Fedrizzi, M. (2011) Communications/Navigation Outage Forecasting System Observational Support for the Equatorial $E \times B$ Drift Velocities Associated with the Four-Cell Tidal Structures. *Radio Science*, **46**, RS0D09. <https://doi.org/10.1029/2010RS004557>
- [2] Hanson, W.B. and Moffett, R.J. (1966) Ionization Transport Effects in the Equatorial F Region. *Journal of Geophysical Research*, **71**, 5559-5572. <https://doi.org/10.1029/JZ071i023p05559>
- [3] Khadka, S.M., Valladares, C.E., Sheehan, R. and Gerrard, A.J. (2018) Effects of Electric Field and Neutral Wind on the Asymmetry of Equatorial Ionization Anomaly. *Radio Science*, **53**, 683-697. <https://doi.org/10.1029/2017RS006428>
- [4] Subhadra Devi, P.K. (2013) Behaviour of Ionosphere and Its Interaction with Solar Magnetosphere System. PhD Thesis, School of Pure and Applied Physics, Mahatma Gandhi University, Ri Bhoi.
- [5] Sultan, P.J. (1996) Linear Theory and Modeling of the Rayleigh-Taylor Instability Leading to the Occurrence of Equatorial Spread F. *Journal of Geophysical Research*, **101**, 26875-26891. <https://doi.org/10.1029/96JA00682>
- [6] Buonsanto, M.J. (1999) Ionospheric Storms—A Review. *Space Science Reviews*, **88**, 563-601. <https://doi.org/10.1023/A:1005107532631>
- [7] Amaechi, P.O., Oyeyemi, E.O., Akala, A.O., Messanga, H.E., Panda, S.K., Seemala, G.K., *et al.* (2021) Ground Based GNSS and C/NOFS Observations of Ionospheric Irregularities over Africa: A Case Study of the 2013 St. Patrick's Day Geomagnetic Storm. *Space Weather*, **19**, e2020SW002631. <https://doi.org/10.1029/2020SW002631>
- [8] Yizengaw, E. and Moldwin, M.B. (2009) African Meridian B-Field Education and Research (AMBER) Array. *Earth, Moon, and Planets*, **104**, 237-246. <https://doi.org/10.1007/s11038-008-9287-2>
- [9] Rastogi, R.G. and Klobuchar, J.A. (1990) Ionospheric Electron Content within the Equatorial F2 Layer Anomaly Belt. *Journal of Geophysical Research*, **95**, 19,045-19,052. <https://doi.org/10.1029/JA095iA11p19045>
- [10] Gonzales, C.A., Kelley, M.C., Fejer, B.G., Vickrey, J.F. and Woodman, R.F. (1979) Equatorial Electric Fields during Magnetically Disturbed Conditions. 2: Implications of Simultaneous Auroral and Equatorial Measurements. *Journal of Geophysical Research: Space Physics*, **84**, 5803-5812. <https://doi.org/10.1029/JA084iA10p05803>
- [11] Kassamba, A.A., Doumbia, V., Obrou, O.K., *et al.* (2020) Estimating the Daytime Vertical $E \times B$ Drift Velocities in F-Region of the Equatorial Ionosphere Using the IEEY and AMBER Magnetic Data in West Africa. *Advances in Space Research*, **65**, 2573-2585. <https://doi.org/10.1016/j.asr.2020.03.008>
- [12] Anderson, D.N., Anghel, A., Yumoto, K., Ishitsuka, M. and Kudeki, E. (2002) Estimating Daytime, Vertical $E \times B$ Drift Velocities in the Equatorial F-Region Using Ground-Based Magnetometer Observations. *Geophysical Research Letters*, **29**, 37-

- 1-37-4. <https://doi.org/10.1029/2001GL014562>
- [13] Anderson, D.N., Anghel, A., Chau, J. and Veliz, O. (2004) Daytime Vertical $E \times B$ Drift Velocities Inferred from Ground-Based Magnetometer Observations at Low Latitudes. *Space Weather*, **2**, S11001. <https://doi.org/10.1029/2004SW000095>
- [14] Yizengaw, E., Moldwin, M.B., Zesta, E., Biouele, C.M., Damtie, B., *et al.* (2014) The Longitudinal Variability of Equatorial Electrojet and Vertical Drift Velocity in the African and American Sectors. *Annals of Geophysics*, **32**, 231-238. <https://doi.org/10.5194/angeo-32-231-2014>
- [15] Akala, A.O., Seemala, G.K., Doherty, P.H., Valladares, C.E., Carrano, C.S., Espinoza, J. and Oluyo, S. (2013) Comparison of Equatorial GPS-TEC Observations over an African Station and an American Station during the Minimum and Ascending Phases of Solar Cycle 24. *Annals of Geophysics*, **31**, 2085-2096. <https://doi.org/10.5194/angeo-31-2085-2013>
- [16] Amaechi, P.O., Oyeyemi, E.O. and Akala, A.O. (2018) Geomagnetic Storm Effects on the Occurrences of Ionospheric Irregularities over the African Equatorial/Low-Latitude Region. *Advances in Space Research*, **61**, 2070-2090. <https://doi.org/10.1016/j.asr.2018.01.035>
- [17] Paznukhov, V., Carrano, V., Doherty, C.S., Groves, P.H., Caton, K.M., Valladares, R.G., *et al.* (2012) Equatorial Plasma Bubbles and L-Band Scintillations in Africa during Solar Minimum. *Annales Geophysicae*, **30**, 675-682. <https://doi.org/10.5194/angeo-30-675-2012>
- [18] Mungufeni, P., Habarulema, J.B. and Jurua, E. (2016) Trends of Ionospheric Irregularities over African Low Latitude Region during Quiet Geomagnetic Conditions. *Journal of Atmospheric and Solar Terrestrial Physics*, **138**, 261-267. <https://doi.org/10.1016/j.jastp.2016.01.015>
- [19] Yizengaw, E. (2021) Ionospheric Dynamics and Their Strong Longitudinal Dependences, Space Physics and Aeronomy Collection Volume 3: Ionosphere Dynamics and Applications. Geophysical Monograph 260, American Geophysical Union, John Wiley & Sons, Inc., Hoboken. <https://doi.org/10.1002/9781119815617.ch17>
- [20] Beaujardiére, O. and the C/NOFS Science Definition Team (2004) C/NOFS: A Mission to Forecast Scintillations. *Journal of Atmospheric and Solar-Terrestrial Physics*, **66**, 1573-1591. <https://doi.org/10.1016/j.jastp.2004.07.030>
- [21] Drob, D.P., Emmert, J.T., Meriwether, J.W., Makela, J.J., Doornbos, E., Conde, M. and Klenzing, J.H. (2015) An Update to the Horizontal Wind Model (HWM): The Quiet Time Thermosphere. *Earth and Space Science*, **2**, 301-319. <https://doi.org/10.1002/2014EA000089>
- [22] Honoré, M.E., Anad, F., Marie, N.C. and César, M.B. (2017) Sq(H) Solar Variation at Yaoundé-Cameroon AMBER Station from 2011 to 2014. *International Journal of Geosciences*, **8**, 545-562.
- [23] Yizengaw, E., Moldwin, M.B., Mebrahtu, A., Damtie, B., Zesta, E., Valladares, C.E. and Doherty, P. (2011) Comparison of Storm Time Equatorial Ionospheric Electrodynamics in the African and American Sector. *Journal of Atmospheric and Solar-Terrestrial Physics*, **73**, 156-163. <https://doi.org/10.1016/j.jastp.2010.08.008>
- [24] Yizengaw, E., Zesta, E., Moldwin, M.B., Damtie, B., Mebrahtu, A., *et al.* (2012) Longitudinal Differences of Ionospheric Vertical Density Distribution and Equatorial Electrodynamics. *Journal of Geophysical Research*, **117**, A07312. <https://doi.org/10.1029/2011JA017454>
- [25] Scherliess, L. and Fejer, B.G. (1999) Radar and Satellite Global Equatorial F-Region Vertical Drift Model. *Journal of Geophysical Research*, **104**, 6829-6842.

- <https://doi.org/10.1029/1999JA900025>
- [26] Manoj, C. and Maus, S. (2012) A Real-Time Forecast Service for the Ionospheric Equatorial Zonal Electric Field. *Space Weather*, **10**, S09002. <https://doi.org/10.1029/2012SW000825>
- [27] Kaab, M., Benkhaldoun, Z., Fisher, D.J., Harding, B., Bounhir, A., Makela, J.J., *et al.* (2017) Climatology of Thermospheric Neutral Winds over Oukaimeden Observatory in Morocco. *Annales Geophysicae*, **35**, 161-170. <https://doi.org/10.5194/angeo-35-161-2017>
- [28] Amaechi, P.O., Oyeyemi, E.O., Akala, A.O., Falayi, E.O., Kaab, M., Benkhaldoun, Z., *et al.* (2020) Quiet Time Ionospheric Irregularities over the African Equatorial Ionization Anomaly Region. *Radio Science*, **55**, e2020RS007077. <https://doi.org/10.1029/2020RS007077>
- [29] Chartier, A.T., Makela, J.J., Liu, H., Bust, G.S. and Noto, J. (2015) Modeled and Observed Equatorial Thermospheric Winds and Temperatures. *Journal of Geophysical Research: Space Physics*, **120**, 5832-5844. <https://doi.org/10.1002/2014JA020921>
- [30] Link, R. and Cogger, L. (1988) A Reexamination of the OI 6300-Å Nightglow. *Journal of Geophysical Research*, **93**, 9883-9892. <https://doi.org/10.1029/JA093iA09p09883>
- [31] Rastogi, R.G. (1994) Westward Equatorial Electrojet during Daytime Hours. *Journal of Geophysical Research*, **79**, 1503-1512. <https://doi.org/10.1029/JA079i010p01503>
- [32] Richmond, A.D. (1995) Ionospheric Electrodynamics Using Magnetic Apex Coordinates. *Journal of Geomagnetism and Geoelectricity*, **47**, 191-212. <https://doi.org/10.5636/jgg.47.191>
- [33] Chapman, S. (1951) The Equatorial Electrojet as Detected from the Abnormal Electric Current Distribution above Huancayo, Peru and Elsewhere. *Archiv für Meteorologie, Geophysik und Bioklimatologie. Serie A*, **4**, 368-390. <https://doi.org/10.1007/BF02246814>
- [34] Anderson, D., Anghel, A., Chau, J.L. and Yumoto, K. (2006) Global, Low-Latitude, Vertical $E \times B$ Drift Velocities Inferred from Daytime Magnetometer Observations. *Space Weather*, **4**, S08003. <https://doi.org/10.1029/2005SW000193>
- [35] Kelley, M.C. (1989) The Earth's Ionosphere, Plasma Physics and Electrodynamics. International Geophysics Series, 43. Academic Press, Inc., Cambridge.
- [36] Rabiú, A.B., Yumoto, K., Falayi, E.O., Bello, O.R. and MAGDAS/CPMN Group (2011) Ionosphere over Africa: Results from Geomagnetic Field Measurements during International Heliophysical Year IHY. *Sun and Geosphere*, **6**, 61-64.
- [37] Rabiú, A.B., Folarin, O.O., Uozumi, T., Hamid, N.S.A. and Yoshikawa, A. (2017) Longitudinal Variation of Equatorial Electrojet and the Occurrence of Its Counter Electrojet. *Annales Geophysicae*, **35**, 535-545. <https://doi.org/10.5194/angeo-35-535-2017>
- [38] West, K.H. and Heelis, R.A. (1996) Longitude Variations in Ion Composition in the Morning and Evening Topside Equatorial Ionosphere near Solar Minimum. *Journal of Geophysical Research*, **101**, 7951-7960. <https://doi.org/10.1029/95JA03377>
- [39] Yamazaki, D., Loughlin, F.O., Trigg, M.A., Miller, Z.F., Pavelsky, T.M. and Bates, P.D. (2014) Development of the Global Width Database for Large Rivers. *Water Resources Research*, **50**, 3467-3480. <https://doi.org/10.1002/2013WR014664>
- [40] Vichare, G. and Richmond, A.D. (2005) Simulation Study of the Longitudinal Variation of Evening Vertical Ionospheric Drifts at the Magnetic Equator during Equinox. *Journal of Geophysical Research—Space Physics*, **110**, A05304.

- <https://doi.org/10.1029/2004JA010720>
- [41] Hagan, M.E. and Forbes, J.M. (2002) Migrating and Nonmigrating Diurnal Tides in the Middle and Upper Atmosphere Excited by Tropospheric Latent Heat Release. *Journal of Geophysical Research*, **107**, ACL 6-1-ACL 6-15.
<https://doi.org/10.1029/2001JD001236>
- [42] Hartman, W.A. and Heelis, R.A. (2007) Longitudinal Variations in the Equatorial Vertical Drift in the Topside Ionosphere. *Journal of Geophysical Research*, **112**, A03305.
<https://doi.org/10.1029/2006JA011773>
- [43] Tesema, F. Mesquita, R., Meriwether, J., Damtie, B., Nigussie, M., Makela, J., *et al.* (2017) New Results on Equatorial Thermospheric Winds and Temperatures from Ethiopia, Africa. *Annales Geophysicae*, **35**, 333-344.
<https://doi.org/10.5194/angeo-35-333-2017>
- [44] Rabiú, A.B., Okoh, D.I., Wu, Q., Bolaji, O.S., Abdulrahim, R.B., Dare-Idowu, O.E. and Obafaye, A.A. (2021) Investigation of the Variability of Nighttime Equatorial Thermospheric Winds over Nigeria, West Africa. *Journal of Geophysical Research: Space Physics*, **126**, e2020JA028528. <https://doi.org/10.1029/2020JA028528>